

Time-lens based multi-color background-free coherent anti-Stokes Raman scattering microscopy

Yifan Qin^{*a,b}, Bo Li^b, Fei Xia^b, Yuanqin Xia^a, Chris Xu^b

^aNational Key Laboratory of Science and Technology on Tunable Laser, Harbin Institute of Technology, 2 Yikuang Street, Harbin, China 150080; ^bSchool of Applied and Engineering Physics, Cornell University, 142 Sciences Drive, Ithaca, NY, USA 14853-2501

ABSTRACT

We demonstrate a multi-color background-free coherent anti-Stokes Raman scattering (CARS) imaging system, using a low-cost, all-fiber, energetic, multi-wavelength time-lens source. The time-lens source generates picosecond pulse trains at three different wavelengths. The first is 1064.3 nm, the second is tunable between 1052 nm and 1055 nm, and the third is tunable between 1040 nm and 1050 nm. When the time-lens source is synchronized with a mode-locked Ti:Sa laser, two of the three wavelengths are used to detect different Raman frequencies for two-color on-resonance imaging, whereas the third wavelength is used to obtain the off-resonance image for nonresonant background subtraction. Mixed poly(methyl methacrylate) (PMMA) and polystyrene (PS) beads are used to demonstrate two-color background-free CARS imaging. Synchronization of the multi-wavelength time-lens source with a microscope enables pixel-to-pixel wavelength-switching. Simultaneous two-color CARS imaging of CH₂ and CH₃ stretching vibration modes with real-time background subtraction is demonstrated in *ex vivo* mouse tissue.

Keywords: coherent anti-Stokes Raman scattering microscopy, multi-color, time-lens, nonresonant background

1. INTRODUCTION

Laser scanning microscopy, which enables non-invasive three-dimensional imaging, has become an invaluable tool for a variety of biological and medical applications¹⁻⁴. Apart from general advantages, coherent anti-Stokes Raman scattering (CARS) microscopy allows label-free and chemically specific imaging of biological samples with endogenous image contrast based on vibrational spectroscopy⁵. A major drawback of CARS is the existence of nonresonant background, which overwhelms resonant signal of Raman peaks, and obscures the contrast of images. Multiple methods have been applied to suppress nonresonant background, including polarization-sensitive detection, time-resolved detection, frequency modulation, and nonlinear interferometric vibrational imaging. These techniques are limited by either resonant signal attenuation or complicated implementation^{6,7}. Temporal synchronization of two picosecond excitation sources, providing the pump and Stokes fields, is a critical requirement in realizing CARS microscopy. Synchronized mode-locked Ti:Sa lasers and optical parametric oscillators (OPOs) are costly and environmentally sensitive, with the need of precise alignment and careful maintenance, and a robust, energetic, and low-cost fiber excitation source for CARS imaging remains a major challenge^{8,9}. In this paper, we demonstrate a cost-effective, energetic, all-fiber, multi-wavelength time-lens source for multi-color background-free CARS imaging. The capability of synchronization with any mode-locked laser is the most appealing advantage of the time-lens source¹⁰⁻¹². Electronic tuning of the pulse delay is used to achieve temporal overlap between the pump and Stokes pulse trains for CARS imaging, eliminating the need of cumbersome mechanical optical delay lines. What's more, a simple and efficient method is applied to remove nonresonant background by digitally subtracting the off-resonance image from the on-resonance image.

2. EXPERIMENTAL SETUP

As shown in Figure 1, the experimental setup can be divided into three parts, *i.e.*, the pump, the Stokes (time-lens source), and the microscope.

*qinyifanhit@gmail.com, yq88@cornell.edu; phone 1 607 255-8034; www.researchgate.net/profile/Yifan_Qin

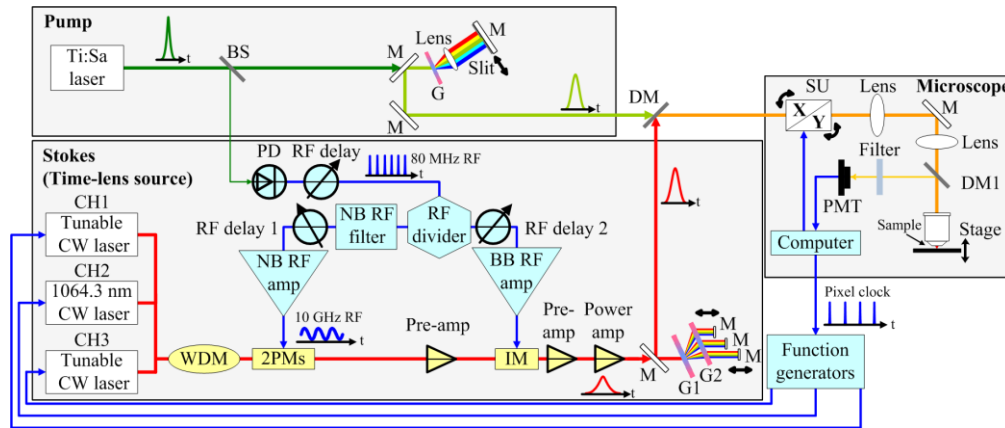


Figure 1. Experimental setup of a multi-wavelength time-lens source (Stokes), synchronized with a mode-locked Ti:Sa laser (pump). The pump light path is shown in green. The Stokes light path is shown in red. The electrical path is shown in blue. BS, beam splitter; M, mirror; G, G1, G2, gratings; DM, DM1, dichroic mirrors; PD, photodiode; WDM, wavelength-division multiplexer; NB, narrowband; BB, broadband; PM, phase modulator; IM, intensity modulator; SU, scan unit; PMT, photomultiplier tube.

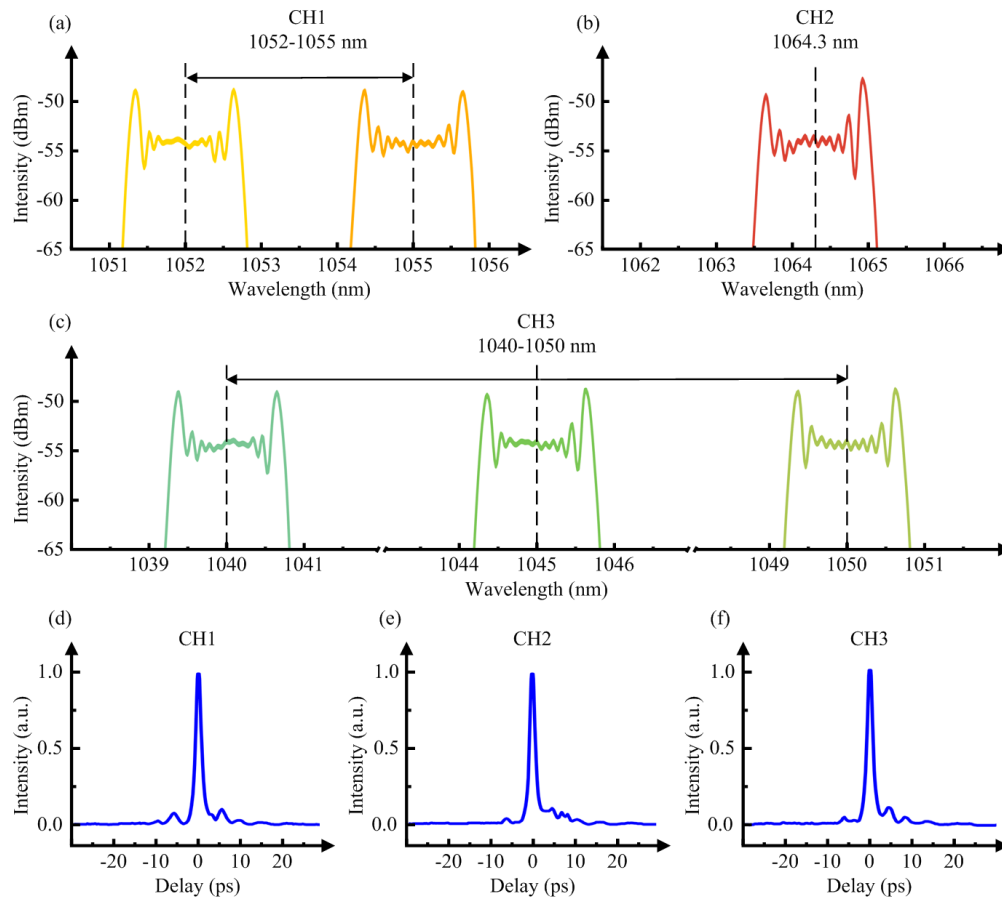


Figure 2. Characterization of the time-lens source. (a) Wavelength tuning range of CH1 is 1052–1055 nm. (b) Wavelength of CH2 is 1064.3 nm. (c) Wavelength tuning range of CH3 is 1040–1050 nm. (d–f) Cross-correlation traces between CH1 (1053.7 nm), CH2 (1064.3 nm), and CH3 (1045.5 nm) of the time-lens source and the spectrally unfiltered 100 fs pulse from the mode-locked Ti:Sa laser.

Femtosecond pulses from a mode-locked Ti:Sa laser (Mai Tai HP DeepSee, Spectra-Physics) are broadened to ~ 1 ps, serving as the pump for CARS imaging. A time-lens source is synchronized with the Ti:Sa laser (pump), serving as the Stokes. A GaAs photodetector (ET-4000, EOT) converts the 80 MHz optical pulse train from the Ti:Sa mode-locked laser to a RF pulse train. One branch of the RF pulse train is filtered by a narrowband filter centered at the 125th harmonic of the 80 MHz repetition rate, with a 3-dB bandwidth of 50 MHz. The resulting 10 GHz sinusoid is amplified to drive two electro-optic phase modulators (2PMs). The other branch is amplified to drive a Mach-Zehnder intensity modulator (IM). A wavelength-tunable distributed-feedback continuous-wave (DFB CW) laser diode, a wavelength-stabilized fiber-Bragg-grating (FBG) CW laser diode, and a wavelength-tunable CW laser diode are, respectively, the sources for the three wavelength channels, CH1, CH2 and CH3, of the time-lens source. After phase modulation by the 2PMs, the IM carves synchronized pulses with temporal widths of 80 ps (full-width-at-half-maximum, FWHM) onto the CW lights. Two pre-amplifiers are used to compensate for the power loss from the PMs and IM. A power amplifier is used to further increase the power. A transmission grating pair is used for dispersion compensation and pulse compression. The pump and the Stokes beams are spatially and temporally overlapped, respectively, by using a dichroic mirror and RF delay lines, and they are sent into a modified laser scanning microscope (FV1000MPE, Olympus) for CARS imaging. When function generators triggered by the pixel clock from the microscope are used to directly modulate the lasers for different channels of the time-lens source, pixel-to-pixel wavelength-switching working mode is achieved, which is essential for simultaneous two-color CARS imaging with real-time background subtraction.

The pump beam has a FWHM spectral bandwidth of ~ 1.8 nm, and a maximum average power of ~ 200 mW. Figures 2(a)–2(c) show the wavelengths of CH1, CH2 and CH3 are 1052–1055 nm, 1064.3 nm and 1040–1050 nm, respectively. All channels of the time-lens source have FWHM spectral bandwidths of ~ 1.5 nm. Cross-correlation is performed between the output of the time-lens source and the spectrally unfiltered 100 fs pulses from the mode-locked Ti:Sa laser. Cross-correlation traces in Figures 2(d)–(f) show the FWHM pulse widths of the time-lens source are ~ 1.9 ps for all channels. In the pixel-to-pixel wavelength-switching working mode, the maximum average power of each channel is ~ 400 mW.

3. RESULTS

We first demonstrate two-color background-free CARS imaging (nonsimultaneous) of a mixture of PMMA (4–13 μm diameters) and PS (2.5–3.5 μm diameters) beads immersed in a 2% agarose gel. The wavelength of the pump is tuned to 803.2 nm, and the wavelengths of the Stokes are tuned to 1052.6 nm (CH1) and 1064.3 nm (CH2). At the focal plane, the pump, CH1 and CH2 of the Stokes (time-lens source) have the average power of 50 mW, 25 mW and 25 mW, respectively. As shown in Figures 3(a) and 3(b), the two-color on-resonance images at Raman frequencies of 2950 cm^{-1} and 3054 cm^{-1} have strong resonant signal with noticeable nonresonant background. The nonresonant background is mainly contributed by the surrounding medium. To perform background-free imaging, the wavelengths of the pump and CH3 of the Stokes are tuned to 809.1 nm and 1046.1 nm to probe Raman frequency at 2800 cm^{-1} . At the focal plane, the average power of pump and Stokes (CH3) are 50 mW and 25 mW, respectively. After subtraction of the off-resonance image Figure 3(c) from the on-resonance images, two-color background-free CARS images are obtained, as shown in Figures 3(d) and 3(e). In Figure 3(d), only PMMA beads contribute to the CARS signal. In Figure 3(e), only PS beads contribute to the CARS signal. The composite of Figures 3(d) and 3(e) is depicted in Figure 3(f), which shows spatial distribution of PMMA beads and PS beads. Figures 3(g) and 3(h) show that the nonresonant background in Figures 3(a) and 3(b) is effectively suppressed after subtraction.

Possible artifact from sample motion is a concern, and thus we demonstrate simultaneous two-color CARS imaging with real-time background subtraction by using excised fresh tissue from a mouse ear. The wavelength of the pump is tuned to 810.7 nm. The wavelengths of the Stokes are tuned to 1053.7 nm (CH1), 1064.3 nm (CH2), and 1045.5 nm (CH3) to probe Raman peak of CH_2 stretching vibration at 2845 cm^{-1} , Raman peak of CH_3 stretching vibration at 2940 cm^{-1} , and off-resonance background at 2770 cm^{-1} , respectively. At the focal plane, the pump, CH1, CH2 and CH3 of the Stokes (the time-lens source) have the average power of 40 mW, 20 mW, 20 mW and 20 mW, respectively. Figure 4(a) is a CARS image of the fresh tissue from the mouse ear, and different columns of the image correspond to different Raman frequencies. Figures 4(b) and 4(c) are zoomed-in images from different regions of Figure 4(a). Zoomed-in illustrations of Figures 4(b) and 4(c) are shown in Figure 4(d), showing adjacent pixels obtained at Raman frequencies of 2845 cm^{-1} , 2940 cm^{-1} and 2770 cm^{-1} . Figures 4(e)–4(g) are CARS images extracted from Figure 4(a), corresponding to Raman frequencies of 2845 cm^{-1} , 2940 cm^{-1} and 2770 cm^{-1} , respectively. As shown in Figures 4(e) and 4(f), two-color on-resonance images have strong resonant signal with noticeable nonresonant background. The nonresonant background is

mainly contributed by the surrounding medium. After subtraction of the off-resonance image Figure 4(g), two-color background-free CARS images are obtained, as shown in Figures 4(h) and 4(i). The nonresonant background is effectively suppressed after subtraction. Lipid and protein are main components of mouse ear tissue, and they both contribute to the CARS signal at 2845 cm^{-1} and 2940 cm^{-1} . The majority of pixels obtained at 2845 cm^{-1} are brighter than the ones obtained at 2940 cm^{-1} in possible lipid-rich region of Figure 4(b), while the majority of pixels obtained at 2940 cm^{-1} are brighter than the ones obtained at 2845 cm^{-1} in possible protein-rich region of Figure 4(c). For the field-of-view shown in Figure 4(a), each pixel is $\sim 200\text{ nm}$ in the sample plane (Figure 4(d)), which is sufficiently small so that the three wavelength channels in adjacent pixels sample approximately the same resolution volume.

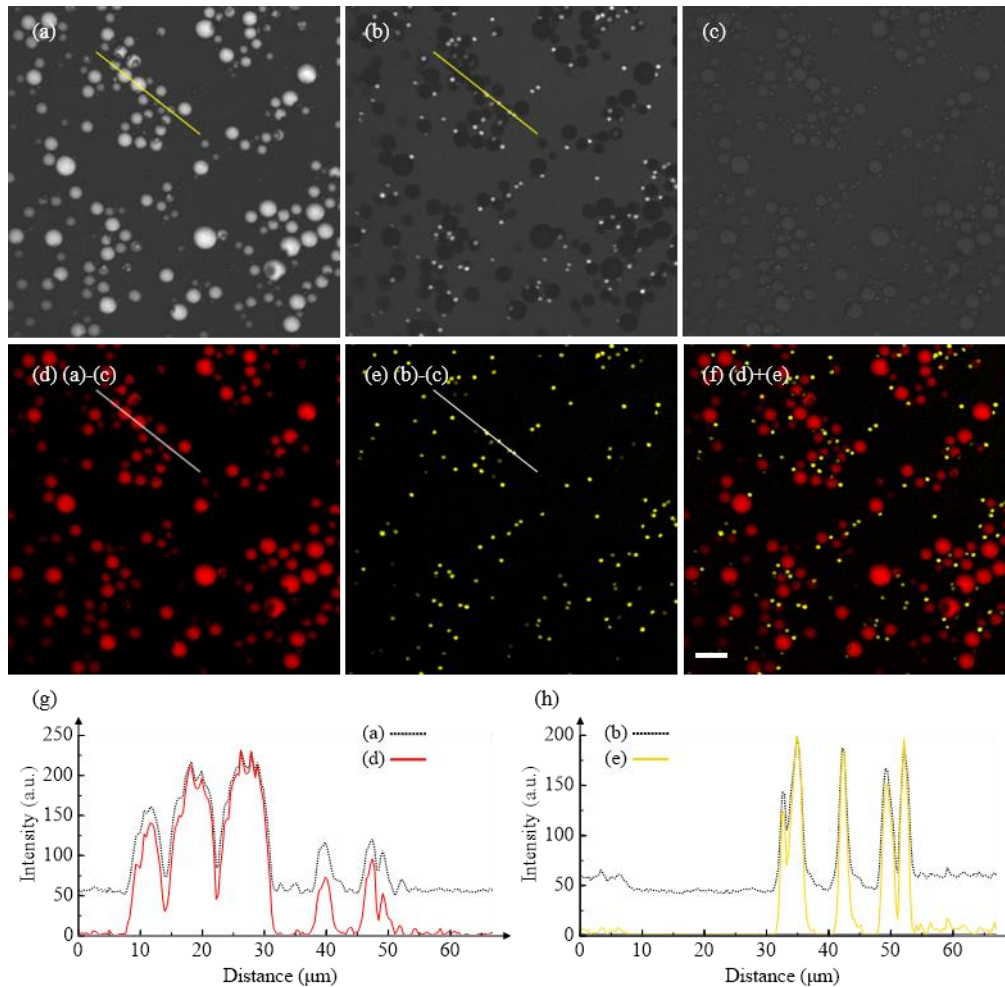


Figure 3. Two-color CARS imaging of mixed PMMA and PS beads, 512×512 pixels, $2\ \mu\text{s}/\text{pixel}$. (a), (b) and (c) are CARS images obtained at Raman frequencies of 2950 cm^{-1} , 3054 cm^{-1} , and 2800 cm^{-1} , respectively. (d–e) Images after subtraction of the off-resonance image (c) from the on-resonance images (a) and (b), achieving background-free images of PMMA beads (red) and PS beads (yellow). Note that the brightness of (d) and (e) is increased by ~ 1.5 times to match the brightness scale of (a) and (b). (f) Composite image of PMMA beads (d) and PS beads (e). (g) shows the corresponding intensity profiles along the line indicated in (a) (dotted black line) and (d) (solid red line). (h) shows the corresponding intensity profiles along the line indicated in (b) (dotted black line) and (e) (solid yellow line). The scale bar is $15\ \mu\text{m}$.

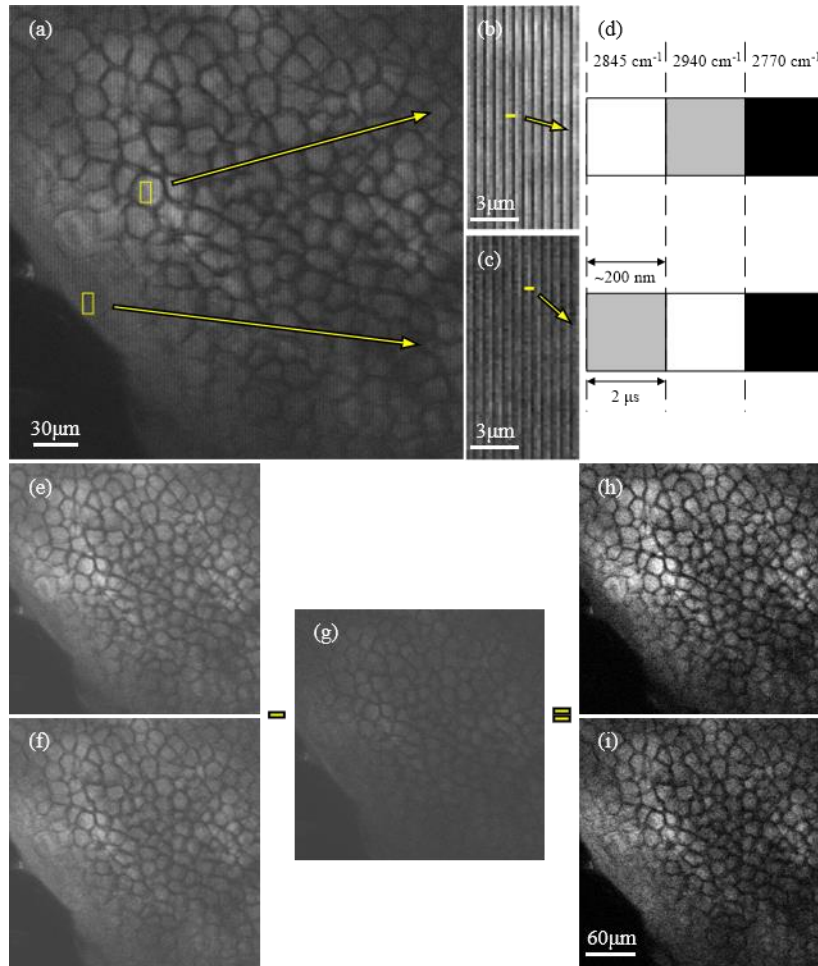


Figure 4. Demonstration of simultaneous two-color CARS imaging with real-time nonresonant background subtraction, 2 $\mu\text{s}/\text{pixel}$, 1536×1536 pixels for (a), 512×512 pixels for (e) to (i). (a) A CARS image of fresh tissue from a mouse ear at a depth of $45 \mu\text{m}$. Signals of Raman frequencies at 2845 cm^{-1} , 2940 cm^{-1} and 2770 cm^{-1} are obtained in different columns of the same image. (b–c) Zoomed-in images from different regions of (a). (d) Zoomed-in views of (b) and (c). (e–g) CARS images extracted from different columns of (a), corresponding to CH_2 stretching vibration (2845 cm^{-1}), CH_3 stretching vibration (2940 cm^{-1}), and the off-resonance background (2770 cm^{-1}), respectively. (h–i) Background-free images obtained after subtraction of the off-resonance image (g) from the on-resonance images of (e) and (f).

4. CONCLUSION

The three-wavelength time-lens source has the advantages of convenient synchronization with any mode-locked laser and microscope pixel clock in a robust, cost-effective, all-fiber configuration. The time-lens source generates three picosecond pulse trains at $1052\text{--}1055 \text{ nm}$, 1064.3 nm and $1040\text{--}1050 \text{ nm}$, which are synchronized with the mode-locked laser. Function generators externally triggered by the microscope directly modulate the CW lasers of the three channels of the time-lens source, achieving pixel-to-pixel wavelength-switching, and thus realizing simultaneous two-color CARS imaging with real-time nonresonant background subtraction. The use of the electronic RF delay line to overlap the pump and the Stokes and only one PMT for all three channels greatly simplifies the implementation complexity of multi-color, background-free CARS imaging. The demonstrated time-lens source is analogous to a multi-wavelength telecom transmitter with phase and amplitude modulation, and allows the addition of even more channels with low cost CW lasers and function generators. While not demonstrated in this paper, time-lens sources have been used to perform SRS imaging with high detection sensitivity in our previous work¹⁰. Therefore, CARS imaging with more colors or multiplex SRS imaging could be performed using the time-lens source.

REFERENCES

- [1] Xia, F., Wu, C., Sinefeld, D., Li, B., Qin, Y. and Xu, C., “*In vivo* label-free confocal imaging of the deep mouse brain with long-wavelength illumination,” *Biomed. Opt. Express* 9(12), 6545-6555 (2018).
- [2] Wang, T., Ouzounov, D.G., Wu, C., Horton, N.G., Zhang, B., Wu, C.-H., Zhang Y, Schnitzer, M.J. and Xu, C., “Three-photon imaging of mouse brain structure and function through the intact skull,” *Nat. Methods* 15, 789-792 (2018).
- [3] Qin, Y., Li, Q., Xia, Y., Liu, B. and Zhang, S., “Construction and application of femtosecond laser two-photon fluorescence microscopy system,” *Journal of Harbin Institute of Technology* 47(11), 1-5 (2015).
- [4] Wang, S., Qin, Y., Guo, M., Zhang, S. and Xia, Y., “High speed 3D two-photon fluorescence microscopy by femtosecond laser pulses,” *Proc. SPIE* 10605, 106053J (2017).
- [5] Zumbusch A., Holtom, G.R. and Xie, X.S., “Three-dimensional vibrational imaging by coherent anti-Stokes Raman scattering,” *Phys. Rev. Lett.* 82(20), 4142-4145 (1999).
- [6] Lu, F., Zheng, W., Sheppard, C. and Huang, Z., “Interferometric polarization coherent anti-Stokes Raman scattering (IP-CARS) microscopy,” *Opt. Lett.* 33(6), 602-604 (2008).
- [7] Lee, Y.J. and Cicerone, M.T., “Vibrational dephasing time imaging by time-resolved broadband coherent anti-Stokes Raman scattering microscopy,” *Appl. Phys. Lett.* 92(4), 041108 (2008).
- [8] Kieu, K., Saar, B.G., Holtom, G.R., Xie, X.S. and Wise, F.W., “High-power picosecond fiber source for coherent Raman microscopy,” *Opt. Lett.* 34(13), 2051-2053 (2009).
- [9] Pegoraro, A.F., Ridsdale, A., Moffatt, D.J., Jia, Y., Pezacki, J.P. and Stolow, A., “Optimally chirped multimodal CARS microscopy based on a single Ti:sapphire oscillator,” *Opt. Express* 17(4), 2984-2996 (2009).
- [10] Wang, K., Zhang, D., Charan, K., Slipchenko, M.N., Wang, P., Xu, C. and Cheng, J.-X., “Time-lens based hyperspectral stimulated Raman scattering imaging and quantitative spectral analysis,” *J. Biophotonics* 6(10), 815-820 (2013).
- [11] Li, B., Charan, K., Wang, K., Rojo, T., Sinefeld, D. and Xu, C., “Nonresonant background suppression for coherent anti-Stokes Raman scattering microscopy using a multi-wavelength time-lens source,” *Opt. Express* 24(23), 26687-26695 (2016).
- [12] Qin, Y., Li, B., Xia, F., Xia, Y. and Xu, C., “Multi-color background-free coherent anti-Stokes Raman scattering microscopy using a time-lens source,” *Opt. Express* 26(26), 34474-34483 (2018).